Inorganic Chemistry
Article

Inorg. Chem. 2010, 49, 2247–2258 2247
DOI: 10.1021/ic9021036

Spectroscopic Characterization of Alumina-Supported Bis(allyl)iridium Complexes: Site-Isolation, Reactivity, and Decomposition Studies

Ryan J. Trovitch,[†] Neng Guo,[‡] Michael T. Janicke,[†] Hongbo Li,[†] Christopher L. Marshall,[‡] Jeffrey T. Miller,[‡] Alfred P. Sattelberger,*[,§] Kevin D. John,*[,†] and R. Thomas Baker*[,†,⊥]

[†]*Chemistry Division, Los Alamos National Laboratory, Los Alamos, New Mexico 87545,* [‡]*Chemical Sciences and Engineering Division, Argonne National Laboratory, Argonne, Illinois 60439,* [§]*Energy Sciences and Engineering Directorate, Argonne National Laboratory, Argonne, Illinois 60439, and* [⊥]*Centre for Catalysis Research and Innovation and Department of Chemistry, University of Ottawa, Ottawa, Ontario K1N 6N5, Canada*

Received October 23, 2009

The covalent attachment of tris(allyl)iridium to partially dehydroxylated γ-alumina is found to proceed via surface hydroxyl group protonation of one allyl ligand to form an immobilized bis(allyl)iridium moiety, (≡AlO)Ir(allyl)$_2$, as characterized by CP-MAS ^{13}C NMR, inductively coupled plasma-mass spectrometry, and Ir L_3 edge X-ray absorption spectroscopy. Extended X-ray absorption fine-structure (EXAFS) measurements taken on unsupported Ir(allyl)$_3$ and several associated tertiary phosphine addition complexes suggest that the η^3-allyl ligands generally account for an Ir−C coordination number of 2 rather than 3, with an average Ir−C distance of 2.16 Å. Using this knowledge, combined EXAFS and X-ray absorption near-edge structure studies reveal that a small amount of Ir^0 is also formed upon reaction of Ir(allyl)$_3$ with the surface. It was found that the addition of either 2,6-dimethylphenyl isocyanide or carbon monoxide to the supported complex allows spectroscopic identification of the supported bis(allyl)iridium complexes, (≡AlO)Ir(allyl)$_2$(CNAr) [Ar = 2,6-(CH$_3$)$_2$C$_6$H$_4$] and (≡AlO)Ir(allyl)$_2$(CO)$_2$, respectively. Although samples of the supported bis(allyl)iridium complex are active for the dehydrogenation of cyclohexane to benzene at temperatures between 180 and 220 °C, in situ temperature-programmed reaction XAFS and continuous-flow reactor studies suggest that Ir^0 nanoparticles, rather than a well-defined Ir^{3+} complex, are responsible for the observed activity.

Introduction

While both homogeneous[1] and heterogeneous[2] catalysts have been invaluable to a wide array of industrial processes, they each possess specific advantages that warrant their application in a given transformation. For example, heterogeneous catalysts are generally easy to recycle[3] and tend to be fairly robust, making them ideal for transformations that require elevated temperatures.[2,4] On the other hand, homogeneous catalysts are often easier to analyze spectroscopically and can be readily tuned for increased selectivity or activity through modification of the ligand environment.[5] At the interface between homogeneous and heterogeneous catalysis, efforts to graft well-defined organometallic precatalysts onto solid surfaces have multiplied rapidly over the past decade.[6] This "heterogenization" of homogeneous catalysts can improve their recyclability and stability, by limiting bimolecular decomposition pathways, and enable tuning of the ligand environment either before or after site isolation of the organometallic moiety.

There are several well-investigated methods of covalently tethering an organometallic complex to a surface; however, these approaches can usually be placed into one of two categories. The first category involves binding of the metal complex to an electron-donating functional group, such as a phosphine or N-heterocyclic carbene, which is already attached to the surface. Notably, this methodology has proven

*To whom correspondence should be addressed. E-mail: asattelberger@anl.gov (A.P.S.), kjohn@lanl.gov (K.D.J.), rbaker@uottawa.ca (R.T.B.).

(1) Cornils, B.; Herrmann, W. A. *J. Catal.* **2003**, *216*, 23–31.
(2) Weissermel, K.; Arpe, H.-J. *Industrial Organic Chemistry*; Wiley-VCH: Weinheim, Germany, 2003.
(3) Thomas, J. M.; Raja, R. *Top. Catal.* **2006**, *40*, 3–17.
(4) Guzman, J.; Gates, B. C. *Dalton Trans.* **2003**, 3303–3318.
(5) (a) Hegedus, L. S. *Transition Metals in the Synthesis of Complex Organic Molecules*; University Science Books: Mill Valley, CA, 1999. (b) Parshall, G. W.; Ittel, S. D. *Homogeneous Catalysis: The Applications and Chemistry of Catalysis by Soluble Transition Metal Complexes*; John Wiley & Sons: New York, 1992. (c) Jäkel, C.; Paciello, R. *Chem. Rev.* **2006**, *106*, 2912–2942.
(6) (a) Gates, B. C. In *Catalyst Preparation*; Regalbuto, J. R., Ed.; Taylor & Francis Publishing Group, CRC Press: New York, 2007; Chapter 10, pp 237−249. (b) Severn, J. R.; Chadwick, J. C.; Duchateau, R.; Friedrichs, N. *Chem. Rev.* **2005**, *105*, 4073–4147. (c) Copéret, C.; Chabanas, M.; Saint-Arroman, R. P.; Basset, J.-M. *Angew. Chem., Int. Ed.* **2003**, *42*, 156–181.

Published on Web 01/29/2010

to be successful for the site isolation of olefin metathesis catalysts,[7] as well as several precious metal-based asymmetric hydrogenation[8] and transfer hydrogenation catalysts.[9] The second category includes cases where a reaction takes place between the metal complex and the surface such that salt metathesis or ligand protonation occurs, often resulting in the formation of a metal−oxygen bond. Several advances using this approach have been reported,[7,10] with one notable example being the preparation of a silica-supported tantalum hydride species that is an active catalyst for alkane metathesis.[11] This catalyst was prepared upon silanol protonation of one or two neopentyl groups from $Ta(CH_2C(CH_3)_3)_3(=CHC(CH_3)_3)$, followed by hydrogenation of the reaction mixture. Although it was not the first report of alkane metathesis,[12] Basset's system was the first to rely on a single catalyst to effect this transformation, and turnover numbers as high as 62 were realized for the conversion of butane into other hydrocarbons.

This research sparked further interest in developing an alkane metathesis process that could be used to upgrade low-molecular-weight alkanes into a suitable transportation fuel on a large scale, which could have a significant impact when coupled with the Fischer−Tropsch process.[13] A recent approach to this problem, developed by the Goldman and Brookhart groups,[14] utilized homogeneous iridium pincer dehydrogenation catalysts[15] in tandem with either a Schrock-type[16] or a heterogeneous rhenium oxide[17] olefin metathesis catalyst to obtain a wide distribution of linear alkanes from *n*-decane. Initially, the authors sought to use Grubbs-type olefin metathesis catalysts;[18] however, they determined that these complexes quickly deactivated the iridium dehydrogenation catalysts.[14] Additionally, the authors reported that the rate of alkane metathesis had decreased as a function of time when the molybdenum alkylidene catalysts[16] were employed. When Re_2O_7/Al_2O_3 was ultimately chosen as the olefin metathesis catalyst, it was unclear as to whether the iridium-based dehydrogenation catalyst had been adsorbed onto the alumina surface or remained in solution.[14]

Surface-bound iridium complexes have been investigated as catalysts for both alkene hydrogenation[8b,c] and alkane dehydrogenation. Conversion of isopentane to isopentene has been accomplished with several silica-supported iridium complexes;[19] however, these systems require temperatures higher than 300 °C to achieve reasonable conversion (> 5%). Site isolation of the highly active iridium pincer complexes has also recently been accomplished by modification of the *para* position of the ligand pyridyl ring, and their ability to catalyze transfer dehydrogenation reactions has been investigated.[20] Although these complexes are the most active alkane dehydrogenation catalysts known to date, methods of tethering them to a surface have thus far required complicated ligand syntheses.[20]

In this contribution, our research team set out to prepare immobilized, trivalent iridium complexes from easily synthesized starting materials and to study their viability as alkane dehydrogenation catalysts. With these goals in mind, we decided to model our efforts after the well-studied immobilization of $Ir(acac)_3$,[21] $Ir(C_2H_4)_2(acac)$,[22] and $Rh(allyl)_3$,[23] because complexes of this type satisfy our requirement of using a simple molecular synthon. Although the immobilization reactions of $Ir(acac)_3$[24] and $Ir(C_2H_4)_2(acac)$[25] have only recently been reported to proceed through the protonation of one acetylacetonate (acac) ligand, the site isolation of $Rh(allyl)_3$ has been studied for decades and the outcome is known to be highly sensitive to both temperature and the type of support used. The reaction of $Rh(allyl)_3$ (in hexane at ambient temperature) with a silica surface was first investigated by the Schwartz group and was found to result in the formation of a site-isolated bis(allyl)rhodium complex, $(\equiv SiO)Rh(\eta^3\text{-allyl})_2$, along with 1 equiv of propene (eq 1).[26] Foley and co-workers later suggested that $(\equiv SiO)Rh(\eta^3\text{-allyl})_2$ was not the only product formed from this reaction upon investigating its reactivity toward CO and H_2. They proposed that a fraction of the immobilized $(\equiv SiO)Rh(\eta^3\text{-allyl})_2$ was further protonated by neighboring surface hydroxyl groups, resulting in the loss of 2 additional equiv of propene and the formation of $(\equiv SiO)_3Rh$.[27] A different outcome altogether was proposed by the Iwasawa group, whereupon the reaction of $Rh(allyl)_3$ with TiO_2 resulted in

(7) (a) Buchmeiser, M. R. *Chem. Rev.* **2009**, *109*, 303–321. (b) Copéret, C.; Basset, J.-M. *Adv. Synth. Catal.* **2007**, *349*, 78–92.
(8) (a) Liu, G.; Liu, M.; Sun, Y.; Wang, J.; Sun, C.; Li, H. *Tetrahedron: Asymmetry* **2009**, *20*, 240–246. (b) Liu, G.; Yao, M.; Wang, J.; Lu, X.; Liu, M.; Zhang, F.; Li, H. *Adv. Synth. Catal.* **2008**, *350*, 1464–1468. (c) Sahoo, S.; Kumar, P.; Lefebvre, F.; Halligudi, S. B. *J. Catal.* **2008**, *254*, 91–100.
(9) (a) Liu, G.; Yao, M.; Zhang, F.; Gao, Y.; Li, H. *Chem. Commun.* **2008**, 347–349. (b) Jiang, D. M.; Gao, J. S.; Yang, Q. H.; Yang, J.; Li, C. *Chem. Mater.* **2006**, *18*, 6012–6018. (c) Jiang, D. M.; Yang, Q. H.; Yang, J.; Zhang, L.; Zhu, G. R.; Su, W. G.; Li, C. *Chem. Mater.* **2005**, *17*, 6154–6160.
(10) (a) Fujdala, K. L.; Tilley, T. D. *J. Catal.* **2003**, *216*, 265–275. (b) Lefebvre, F.; Thivolle-Cazat, J.; Dufaud, V.; Niccolai, G. P.; Basset, J.-M. *Appl. Catal., A* **1999**, *182*, 1–8.
(11) Vidal, V.; Théolier, A.; Thivolle-Cazat, J.; Basset, J.-M. *Science* **1997**, *276*, 99–102.
(12) Burnett, R. L.; Hughes, T. R. *J. Catal.* **1973**, *31*, 55–64.
(13) Van der Laan, G. P.; Beenackers, A. A. C. M. *Catal. Rev.—Sci. Eng.* **1999**, *41*, 255–318.
(14) Goldman, A. S.; Roy, A. H.; Huang, Z.; Ahuja, R.; Schinski, W.; Brookhart, M. *Science* **2006**, *312*, 257–261.
(15) (a) Gupta, M.; Hagan, C.; Flesher, R. J.; Kaska, W. C.; Jensen, C. M. *Chem. Commun.* **1996**, 2083–2084. (b) Gupta, M.; Hagan, C.; Kaska, W. C.; Cramer, R. E.; Jensen, C. M. *J. Am. Chem. Soc.* **1997**, *119*, 840–841. (c) Göttker-Schnetmann, I.; White, P.; Brookhart, M. *J. Am. Chem. Soc.* **2004**, *126*, 1804–1811. (d) Göttker-Schnetmann, I.; Brookhart, M. *J. Am. Chem. Soc.* **2004**, *126*, 9330–9338. (e) Liu, F.; Pak, E. B.; Singh, B.; Jensen, C. M.; Goldman, A. S. *J. Am. Chem. Soc.* **1999**, *121*, 4086–4087. (f) Zhu, K.; Achord, P. D.; Zhang, X.; Krogh-Jespersen, K.; Goldman, A. S. *J. Am. Chem. Soc.* **2004**, *126*, 13044–13053.
(16) (a) Schrock, R. R. *Chem. Commun.* **2005**, 2773–2777. (b) Schrock, R. R.; Murdzek, J. S.; Bazan, G. C.; Robbins, J.; DiMare, M.; O'Regan, M. *J. Am. Chem. Soc.* **1990**, *112*, 3875–3886.
(17) (a) Ivin, K. J.; Mol, J. C. *Olefin Metathesis and Metathesis Polymerization*; Academic Press: San Diego, 1997. (b) Pariya, C.; Jayaprakash, K. N.; Sarkar, A. *Coord. Chem. Rev.* **1998**, *168*, 1–48.
(18) Grubbs, R. H. *Tetrahedron* **2004**, *60*, 7117–7140.
(19) Böhmer, I. K.; Alt, H. G. *J. Organomet. Chem.* **2009**, *694*, 1001−1010 and references cited therein.
(20) Huang, Z.; Brookhart, M.; Goldman, A. S.; Kundu, S.; Ray, A.; Scott, S. L.; Vicente, B. C. *Adv. Synth. Catal.* **2009**, *351*, 188–206.
(21) For the first reported synthesis of $Ir(acac)_3$, see: Dwyer, F. P.; Sargeson, A. M. *J. Am. Chem. Soc.* **1953**, *75*, 984–985.
(22) For the first reported synthesis of $Ir(C_2H_4)_2(acac)$, see: Van Gaal, H. L. M.; Van der Ent, A. *Inorg. Chim. Acta* **1973**, *7*, 653–659.
(23) For the first reported synthesis of $Rh(allyl)_3$, see: Powell, J.; Shaw, B. L. *Chem. Commun.* **1966**, 323–325.
(24) Silvennoinen, R. J.; Jylhä, O. J. T.; Lindblad, M.; Sainio, J. P.; Puurunen, R. L.; Krause, A. O. I. *Appl. Surf. Sci.* **2007**, *253*, 4103–4111.
(25) (a) Uzun, A.; Bhirud, V. A.; Kletnieks, P. W.; Haw, J. F.; Gates, B. C. *J. Phys. Chem. C* **2007**, *111*, 15064–15073. (b) Uzun, A.; Ortalan, V.; Browning, N. D.; Gates, B. C. *Chem. Commun.* **2009**, *31*, 4657–4659.
(26) Ward, M. D.; Harris, T. V.; Schwartz, J. *J. Chem. Soc., Chem. Commun.* **1980**, 357–359.
(27) Foley, H. C.; DeCanio, S. J.; Tau, K. D.; Chao, K. J.; Onuferko, J. H.; Dybowski, C.; Gates, B. C. *J. Am. Chem. Soc.* **1983**, *105*, 3074–3082.

the liberation of 2 equiv of propene and the sole formation of $(\equiv TiO)_2Rh(\eta^3\text{-allyl})$.[28] These inconsistencies were later investigated in depth by Dufour et al., who determined that the addition of $Rh(allyl)_3$ to either silica, titania, or alumina results in the rapid formation of the surface-bound bis(allyl)rhodium complex, $(\equiv MO)(\equiv MOX)Rh(\eta^3\text{-allyl})_2$ (M = Si, Ti, Al; X = H, Si), with the liberation of 1 equiv of propene (eq 1).[29] These authors proposed a two-site binding to the surface, and when M = Si and X = H, they observed a loss of additional propene due to silanol protonation of a second allyl group at slightly elevated temperatures (80 °C).

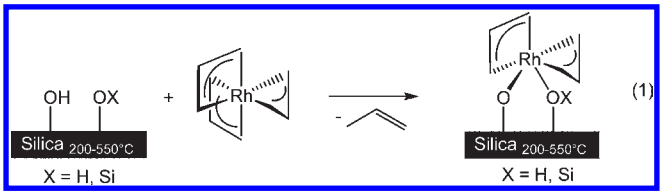

In this paper, we describe our efforts to extend this methodology to the immobilization of $Ir(allyl)_3$ onto partially dehydroxylated γ-alumina and to characterize the resulting site-isolated iridium complex with a combination of spectroscopic methods. Expanding upon our previous studies regarding Lewis base addition to homoleptic metal−allyl complexes,[30,31] the reactivity of this supported complex toward tertiary phosphorus ligands, CO, and 2,6-dimethylphenyl isocyanide is discussed, along with degradation studies and preliminary attempts to catalyze alkane dehydrogenation. We expected that the immobilization of $Ir(allyl)_3$, upon protonation of one or more allyl ligands, would proceed easily based on the successful site isolation of $Rh(allyl)_3$,[26−29] $Ir(acac)_3$,[24] and $Ir(C_2H_4)_2(acac)$.[25] We further expected that supported iridium complexes bearing Lewis base ligands would exhibit better redox stability than the site-isolated rhodium system[32] because $Ir(allyl)_3(L)_n$ complexes have displayed greater stability than their second-row congeners in solution.[30b,33]

Results and Discussion

Preparation and Characterization of the Immobilized Bis(allyl)iridium Moiety. Taking advantage of the previously reported high-yield synthesis of $Ir(allyl)_3$,[30b] our study commenced with the addition of this complex to γ-alumina that had been partially dehydroxylated at either 500 or 1000 °C under a helium flow, as previously described.[34] Upon stirring a pentane slurry of the reactants, a change in color from white to light tan was

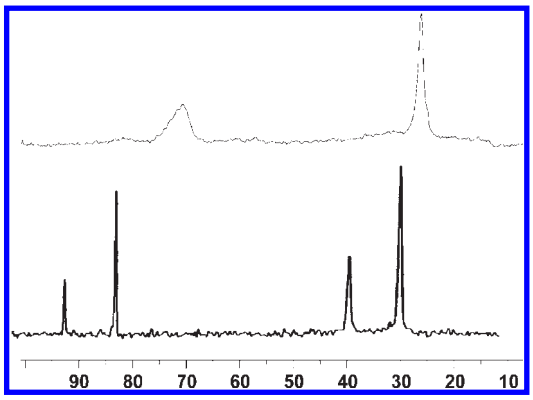

Figure 1. Comparison of the CP-MAS ^{13}C NMR spectra of **1** (top) and $Ir(allyl)_3$ (bottom), in ppm.

observed over the course of 3 days at ambient temperature. At this time, the powder was collected by filtration, washed several times with pentane, and dried in vacuo. Analysis by a variety of spectroscopic methods revealed the formation of the 5-coordinate surface-bound bis(allyl)iridium moiety, $(=AlO)Ir(allyl)_2$ (**1**; eq 2). Although the data collected on **1** discussed below favor this geometry, we cannot definitively rule out the possibility that the iridium center is 6-coordinate, having two surface attachments in a fashion similar to that proposed for the extensively investigated immobilized rhodium complexes, $(\equiv MO)(\equiv MOX)Rh(\eta^3\text{-allyl})_2$ (M = Si, Ti, Al; X = H, Si; eq 1).[29]

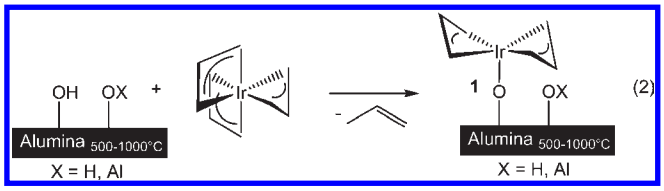

Evaporation of the pentane filtrate in vacuo allowed recollection of up to 20% of the initial $Ir(allyl)_3$, as judged by ^1H NMR spectroscopy upon integration against a known amount of ferrocene. Similar percentages of $Ir(allyl)_3$ recovery were achieved after 5 days under these reaction conditions. Inductively coupled plasma (ICP) analysis of **1** afforded iridium loadings between 1.2 and 1.6 wt %, depending on the batch of γ-alumina employed (due to varying degrees of surface dehydroxylation). Additionally, conducting the immobilization reaction in a J. Young tube with minimal headspace allowed the observation of a stoichiometric amount of propene by ^1H NMR spectroscopy, confirming the loss of one allyl ligand from $Ir(allyl)_3$ upon reaction with the surface (Figure S1, Supporting Information).

In order to obtain valuable structural information about the site-isolated complex, **1**, cross-polarization magic angle spinning (CP-MAS) NMR experiments were conducted. The solid-state ^{13}C NMR spectrum of pure $Ir(allyl)_3$ (Figure 1, bottom) was collected to allow for a comparison with the immobilized material and was found to be consistent with the solution data previously reported for this complex.[35] The CP-MAS ^{13}C NMR

(28) (a) Iwasawa, Y.; Sato, H. *Chem. Lett.* **1985**, 507–510. (b) Tada, M.; Sasaki, T.; Iwasawa, Y. *J. Phys. Chem. B* **2004**, *108*, 2918–2930.
(29) Dufour, P.; Houtman, C.; Santini, C. C.; Nédez, C.; Basset, J. M.; Hsu, L. Y.; Shore, S. G. *J. Am. Chem. Soc.* **1992**, *114*, 4248–4257.
(30) (a) John, K. D.; Salazar, K. V.; Scott, B. L.; Baker, R. T.; Sattelberger, A. P. *Chem. Commun.* **2000**, 581–582. (b) John, K. D.; Salazar, K. V.; Scott, B. L.; Baker, R. T.; Sattelberger, A. P. *Organometallics* **2001**, *20*, 296–304.
(31) Trovitch, R. J.; John, K. D.; Martin, R. L.; Obrey, S. J.; Scott, B. L.; Sattelberger, A. P.; Baker, R. T. *Chem. Commun.* **2009**, 4206–4208.
(32) (a) Santini, C. C.; Scott, S. L.; Basset, J.-M. *J. Mol. Catal. A: Chem.* **1996**, *107*, 263–271. (b) Scott, S. L.; Dufour, P.; Santini, C. C.; Basset, J.-M. *Inorg. Chem.* **1996**, *35*, 869–875. (c) Scott, S. L.; Mills, A.; Chao, C.; Basset, J.-M.; Millot, N.; Santini, C. C. *J. Mol. Catal. A: Chem.* **2003**, *204−205*, 457–463.
(33) Powell, J.; Shaw, B. L. *J. Chem. Soc. A* **1968**, 583–596.
(34) He, M.-Y.; Xiong, G.; Toscano, P. J.; Burwell, R. L., Jr.; Marks, T. J. *J. Am. Chem. Soc.* **1985**, *107*, 641–652.
(35) John, K. D.; Michalczyk, R.; Hernandez, G.; Green, J. C.; Martin, R. L.; Baker, R. T.; Sattelberger, A. P. *Organometallics* **2002**, *21*, 5757–5766.

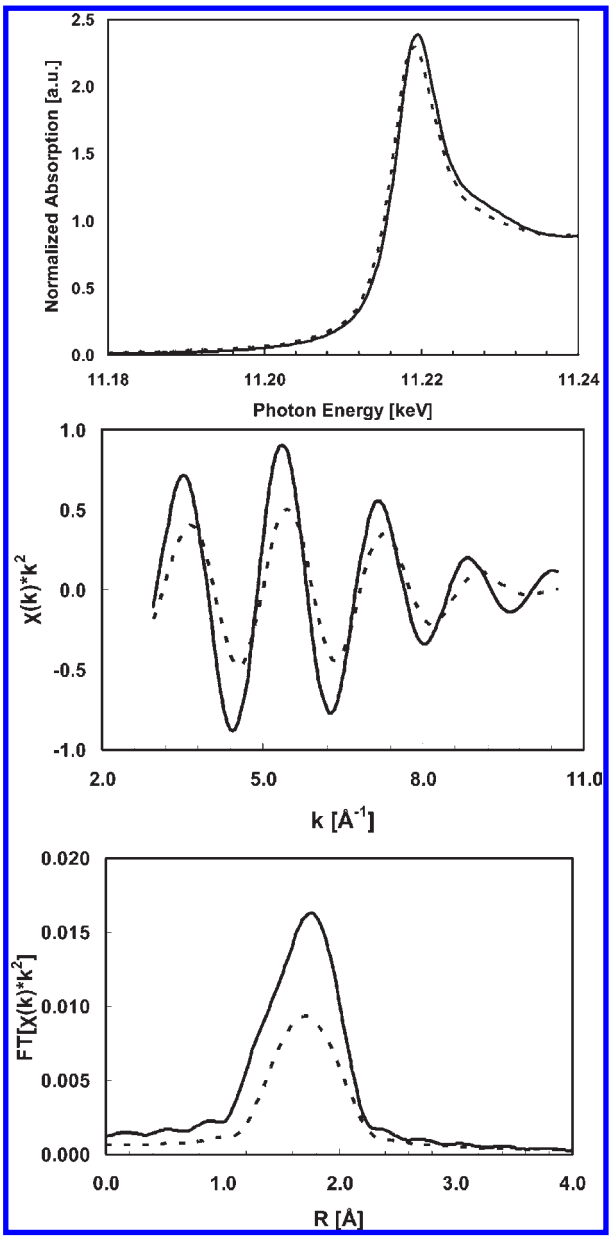

Figure 2. EXAFS data collected for $Ir(allyl)_3$ (solid) and **1** (dashed). At the top is a comparison of the XANES region, displayed alongside the corresponding *k*-space (middle) and *R*-space (bottom; phase correction not applied) plots.

spectrum of **1** (Figure 1, top) was collected over the course of several days (100 000 scans) and was found to exhibit two broad resonances centered at 70.6 ppm (*C*H) and 24.6 ppm (CH_2), consistent with an ensemble of surface-bound species that have two equivalent allyl ligands bound to a 5-coordinate iridium center. The appearance of only two resonances confirms that these allyl ligands are bound in an η^3 fashion because η^1-allyl ligands exhibit three significantly different carbon shifts at approximately 150, 100, and 15 ppm.[30b] On the other hand, we cannot rule out a 6-coordinate species that undergoes rapid, reversible dissociation of a neutral surface oxygen donor in the solid state. The ^{13}C NMR resonances observed for **1** are shifted significantly upfield of the starting material and are reflective of electron donation from the surface oxygen atom with concomitant increased back-bonding to the allyl groups.[36] The ability of this oxygen atom to participate in π-donation to iridium bolsters the formulation of a 5-coordinate metal center in **1** because this type of interaction is present in several reported 5-coordinate iridium(III) complexes.[37] The shifts of the allyl resonances additionally argue against the possibility that **1** is an ion pair with the formula $[Ir(allyl)_2]^+[O{-}Al{=}]^-$. A cationic bis(allyl)iridium complex of this type would be expected to have ^{13}C NMR chemical shifts at a lower field than those observed for $Ir(allyl)_3$.[38]

Table 1. Simulated EXAFS Data for $Ir(allyl)_3$ and the Supported Complexes **1** and **2**

complex	scatter	CN (±20%)	*R* (±0.02 Å)	DWF (Å$^2 \times 10^3$)	E_0 (eV)
$Ir(allyl)_3$	Ir−C	6.8	2.15	5.9	2.0
1	Ir−C/O	3.9	2.13	5.9	2.5
2	Ir−C/O	3.4	2.02	5.9	0.7

Extended X-ray Absorption Fine-Structure (EXAFS) Characterization of Unsupported Tris(allyl)iridium Complexes and 1. To further spectroscopically differentiate $Ir(allyl)_3$ and **1**, EXAFS measurements were carried out on both **1** and a series of unsupported allyliridium complexes. To allow for comparison, XAFS data were first collected on $Ir(allyl)_3$ (Figure 2, solid lines). Identical X-ray absorption near-edge structure (XANES) and *k*-space EXAFS data were collected for this complex upon dilution with either partially dehydroxylated γ-alumina (1000 °C) or boron nitride, providing evidence that a solid-state reaction between $Ir(allyl)_3$ and the γ-alumina hydroxyl groups did not preclude data acquisition. Additionally, exposure of these samples to the beam for extended periods of time did not result in degradation of the complex. Fitting of the EXAFS data of $Ir(allyl)_3$ in *R*-space (Table 1) revealed an Ir−C coordination number of 6.8 at 2.15 Å, rather than the expected value of 9 (3 per η^3-allyl ligand).

Even though determination of the metal−ligand coordination numbers by EXAFS data fitting is a well-established technique, these values can be associated with up to 20% error and bond lengths differing by less than 0.1 Å are difficult to distinguish by this practice.[39] Because the solid-state structure of several related η^3-allyl-ligated iridium complexes feature slightly shorter $Ir{-}C_{methine}$ distances than $Ir{-}C_{methylene}$ distances (by approximately 0.06 Å),[30b] we expected that all nine Ir−C contacts would be accounted for by fitting the major peak at 2.15 Å. However, the fitted coordination number of 6.8 is outside the 20% error range for a molecule with a coordination number of 9. This is not the first time that a lower than expected $M{-}C_{allyl}$ coordination number has been extruded from the EXAFS data fitting of an allyl-ligated organometallic complex. In fact, the fitting of EXAFS data collected on $Rh(allyl)_3$ was previously reported by Iwasawa and co-workers, who determined a

(36) Ahn, H.; Nicholas, C. P.; Marks, T. J. *Organometallics* **2002**, *21*, 1788–1806.
(37) Auburn, M. J.; Holmes-Smith, R. D.; Stobart, S. R.; Bakshi, P. K.; Cameron, T. S. *Organometallics* **1996**, *15*, 3032−3036 and references cited therein.
(38) Wakefield, J. B.; Stryker, J. M. *Organometallics* **1990**, *9*, 2428–2430.
(39) Hsiao, Y.-W.; Tao, Y.; Shokes, J. E.; Scott, R. A.; Ryde, U. *Phys. Rev. B* **2006**, *74*, 214101.

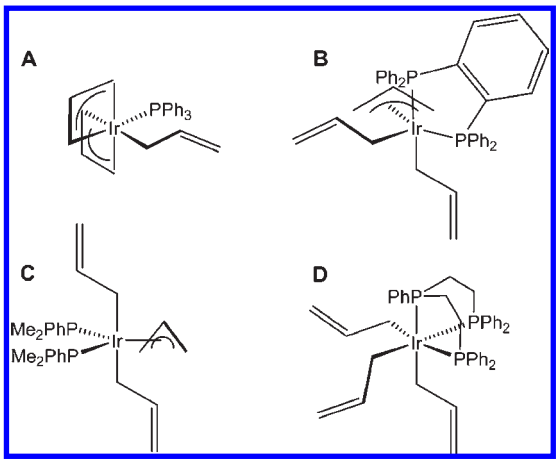

Figure 3. Phosphine-ligated tris(allyl)iridium complexes investigated in this study.

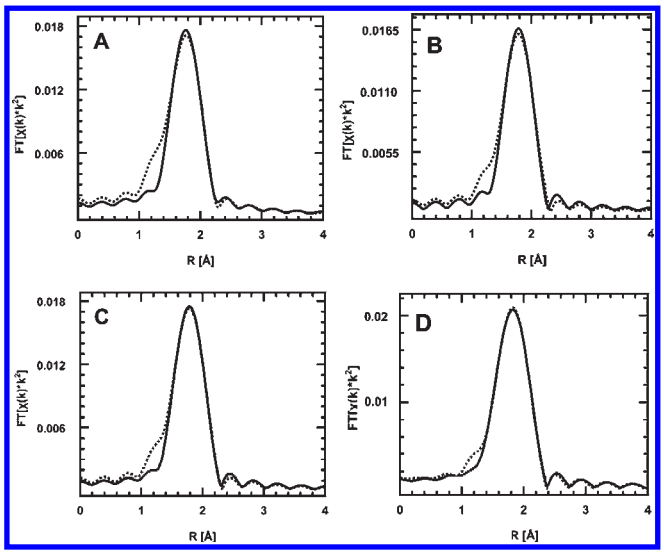

Figure 4. EXAFS data (*R*-space without phase correction, solid lines) collected for **A**−**D**. Corresponding fits are shown with dashed lines.

Rh−C coordination number of 6.7 at 2.18 Å,[28b] values nearly identical with those obtained here for Ir(allyl)$_3$.

Before interpreting the EXAFS spectra of **1**, we sought to further understand this η^3-allyl ligand coordination number phenomenon by fitting the EXAFS data collected on a series of phosphine-ligated tris(allyl)iridium complexes, Ir(allyl)$_3$(PR$_3$)$_n$. The addition of phosphine ligands to Ir(allyl)$_3$ is known to result in tuning of the σ/π-allyl ligand manifold, yielding related tris(allyl) complexes that have different combinations of η^1- and η^3-allyl ligands.[30] The *R*-space EXAFS data (solid lines) collected on four such complexes, Ir(η^3-allyl)$_2$(η^1-allyl)(PPh$_3$) (**A**), Ir(η^3-allyl)(η^1-allyl)$_2$(κ^2-Ph$_2$PC$_6$H$_4$PPh$_2$) (**B**), Ir(η^3-allyl)-(η^1-allyl)$_2$(PMe$_2$Ph)$_2$ (**C**), and Ir(η^1-allyl)$_3$(κ^3-Ph$_2$P(CH$_2$)$_2$-P(Ph)(CH$_2$)$_2$PPh$_2$) (**D**) (Figure 3), along with their respective fits (dashed lines), are illustrated in Figure 4. The Ir−C and Ir−P shells were refined simultaneously to yield the fits that are tabulated in Table 2.

For complex **A**, an Ir−C coordination number of 7 would be expected if each η^3-allyl ligand accounted for three contacts, a number that is within 20% error of the fitted value of 6.5. This value is also just outside the 20% error range expected for a coordination number of 5, which is based on the assumption that each η^3-allyl ligand contributes two Ir−C contacts. The determined Ir−C distance of 2.17 Å is also in good agreement with the metrical parameters previously reported for the solid-state structure of this complex:[30b] Ir−C$_{\sigma\text{-allyl}}$ = 2.167(4) Å; Ir−C$_{\pi\text{-allyl}}$ = 2.145[5] and 2.217[5] Å, for the methine and methylene carbon atoms, respectively. Even though the fitting yielded reasonable E_0 values, it is important to note that the Ir−P distance of 2.44 Å is significantly longer than the experimentally determined value of 2.311(1) Å.

Fitting the EXAFS data of the other phosphine complexes (**B**−**D**) gave simulated Ir−C contact numbers of 4.0, 4.6, and 3.5, respectively. For complexes **B** and **C**, the fitted values are consistent with each η^3-allyl ligand contributing two Ir−C contacts and each η^1-allyl ligand contributing only the α-carbon contact. Similarly, the Ir−C coordination number of 3.5 obtained for **D** is within the 20% error range expected for a value of 3 (for three η^1-allyl ligands). The solid-state structures of complexes **B** and **D** have previously been reported, and in both cases, the fitted Ir−C distances (2.16 and 2.15 Å) are slightly shorter than the average experimental Ir−C values.[30b] Similar to complex **A**, the fitted Ir−P distances obtained for **B** and **D** of 2.40 and 2.42 Å, respectively, are significantly longer than their average X-ray crystallographically determined distances of 2.2783[6] and 2.324[1] Å, respectively.

It is worth mentioning here recent work to deconvolute the EXAFS data collected for [(Ph$_2$PCH$_2$CH$_2$-PPh$_2$)Pd(CH$_2$CHCMe$_2$)][O$_3$SCF$_3$]. The original EXAFS data analysis by Tromp et al. was conducted such that the Pd−C and Pd−P shells were refined separately, leading the authors to report false minima and propose that the allyl ligand in this complex adopts an η^2-hapticity in solution.[40] In the follow-up comprehensive density functional theory and EXAFS modeling study,[41] Caulton and co-workers explained that multiple minima could be arrived at for this complex because the Pd−C and Pd−P EXAFS oscillations are out-of-phase; therefore, small changes in the Pd−C coordination number can be compensated for by changes in the Pd−P coordination number and bond length. For the previously discussed phosphine-ligated iridium complexes, we believe that a similar interplay between the Ir−C coordination number and the Ir−P contact distance could be the reason that we observe longer than expected Ir−P distances when the number of Ir−P contacts is fixed during the EXAFS fitting. Unfortunately, this explanation does not reveal why lower than expected π-allyl coordination numbers have been obtained for Rh(allyl)$_3$[28b] and Ir(allyl)$_3$.

Upon immobilization, a decrease in the absorption edge white line intensity of the iridium moiety was observed (Figure 2, top), which is consistent with a reduction in the coordination number. Similar differences between the supported and unsupported complexes can also be seen in the *k*-space (middle) and *R*-space (bottom) plots, displayed in Figure 2. Importantly, the photon energy at the absorption edge was slightly lower than that

(40) Tromp, M.; van Bokhoven, J. A.; van Haaren, R. J.; van Strijdonck, G. P. F.; van der Eerden, A. M. J.; van Leeuwen, P. W. N. M.; Koningsberger, D. C. *J. Am. Chem. Soc.* **2002**, *124*, 14814–14815.
(41) Clot, E.; Eisenstein, O.; Weng, T.-C.; Penner-Hahn, J.; Caulton, K. G. *J. Am. Chem. Soc.* **2004**, *126*, 9079–9084.

Table 2. EXAFS Fitting Results for **A**−**D** with Fixed Ir−P Coordination Numbers[a]

complex	scatter	expected CN	CN (±20%)	R (±0.02 Å)	DWF (Å^2 × 10^3)	E_0 (eV)
A	Ir−C	5	6.5	2.17	5.9	2.6
	Ir−P	1	1.0	2.44	2.4	5.6
B	Ir−C	4	4.0	2.16	5.9	1.8
	Ir−P	2	2.0	2.40	2.4	1.1
C	Ir−C	4	4.6	2.17	5.9	1.8
	Ir−P	2	2.0	2.41	2.4	1.3
D	Ir−C	3	3.5	2.15	5.9	1.7
	Ir−P	3	3.0	2.42	2.4	−0.1

[a] Expected CN values were calculated considering that each η^3-allyl ligand contributes two Ir−C contacts.

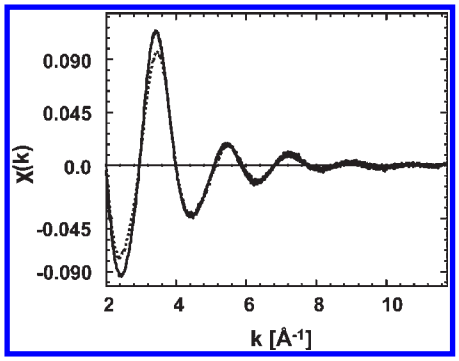

Figure 5. EXAFS data for **1** both before (solid line) and after (dashed line) treatment with PPh_3, shown in the k-space.

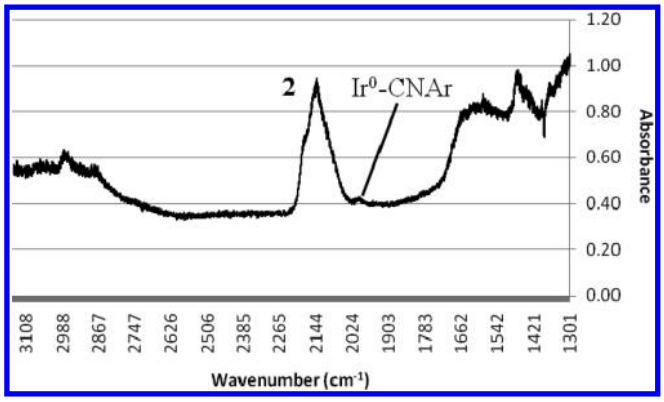

Figure 6. IR spectrum of complex **2**.

observed for the parent complex (Figure 2, top), suggesting that while the majority of iridium centers remain in the 3+ oxidation state upon tethering to the surface, *the reduction of a small percentage of* Ir^{3+} *to* Ir^0 *likely occurs*. Because the percentage of Ir^0 formed is relatively small, a well-defined Ir−Ir shell could not be identified in the k-space or R-space plots of this sample. The formation of some Ir^0 also explains the lower than expected Ir−C/O coordination number of 3.9 at an average bond distance of 2.13 Å. It was expected that upon immobilization a coordination number of approximately 5 (or 6, assuming two Ir−O surface contacts) would be reached, with each allyl ligand contributing two contacts [based on what was observed for $Ir(allyl)_3$]. The Ir−C and Ir−O contacts could not be effectively separated in the data fitting (less than 0.1 Å apart),[39] and all attempts to input a shorter or longer Ir−O bond distance resulted in abnormal threshold energies.

Having already ruled out alternative origins for the low Ir−C/O coordination number observed, such as the formation of an electrostatically surface-bound, 14-electron $[Ir(allyl)_2]^+$ complex or loss of an additional allyl ligand as propene to form a bis(oxido) surface linkage as reported for the Rh congener,[28] formation of a small amount of Ir^0 appears to be the likeliest source for this phenomenon. Having established the identity of **1** through solid-state NMR and EXAFS studies, the reactivity of this complex toward Lewis bases was investigated in order to tune the σ/π-allyl ligand manifold of the supported iridium complex and definitively detect Ir^0 formation.

Reactivity of (=AlO)Ir(allyl)$_2$ toward Lewis Bases. In contrast to the reactivity of $Ir(allyl)_3$ and even some reports on the supported rhodium congener, the addition of tertiary phosphorus ligands to complex **1** did not proceed readily. The addition of a large excess of PPh_3 (15 equiv, based on the iridium content determined by ICP) to **1** at ambient temperature for 2 h and subsequent analysis of the surface by CP-MAS ^{31}P NMR spectroscopy revealed only a resonance at 5 ppm consistent with the formation of [H−PPh_3][O−Al].[42] This resonance was also observed upon the addition of $Ir(allyl)_3(PPh_3)$ to γ-alumina that was partially dehydroxylated at 1000 °C. To verify this lack of PPh_3 affinity, EXAFS data were also collected on **1** after treatment with excess PPh_3 (Figure 5). Similar results were obtained from the addition of $Ir(allyl)_3(PMe_2Ph)_2$ to γ-alumina or treatment of **1** with 20 equiv of the tied-back phosphite $P(OCH_2)_3CCH_3$ for 4 days.

Because definitive IR spectral assignments could not be made on **1** [Ir−X (X = C, O) or C−H bands not discretely identified at high resolution (0.5 cm^{-1}, 128 scans) because of the complexity of the surface and low iridium content], modification of the immobilized bis(allyl)iridium complex with ligands that typically have strong vibrational signatures such as CO and 2,6-dimethylphenyl isocyanide was explored. In solution, $Ir(allyl)_3$ is known to bind 3 equiv of 2,6-dimethylphenyl isocyanide to form $Ir(\sigma\text{-allyl})_3(CNAr)_3$ [Ar = 2,6-$(CH_3)_2C_6H_4$].[30b] Our investigation of this substrate commenced with the addition of 1 equiv of 2,6-dimethylphenyl isocyanide dissolved in pentane to **1**, allowing the formation of (=AlO)Ir(allyl)$_2$(CNAr) (**2**) after 3 days at ambient temperature (eq 3). Upon mixing of the reactants, the γ-alumina changed from light tan to light orange. The IR spectrum of **2** featured a broad band at 2132 cm^{-1} (Figure 6), shifted 15 cm^{-1} from the free isocyanide stretch of 2117 cm^{-1}. In contrast to the previously explored solution chemistry,[30b] **2** was also formed when 20 or 100 equiv of isocyanide was added under these reaction conditions, as judged by EXAFS, CP-MAS ^{13}C NMR, and IR spectroscopy. Binding of more than 1 equiv in this case is likely

(42) Hu, B.; Gay, I. D. *J. Phys. Chem. B* **2001**, *105*, 217–219.

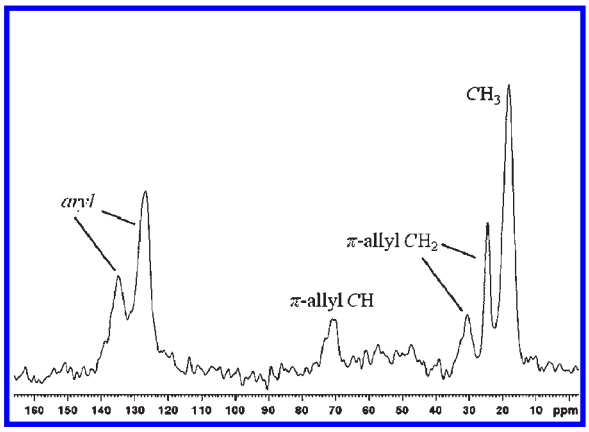

Figure 7. CP-MAS ^{13}C NMR spectrum of **2**, in ppm.

prevented by the steric protection imparted by the surface.

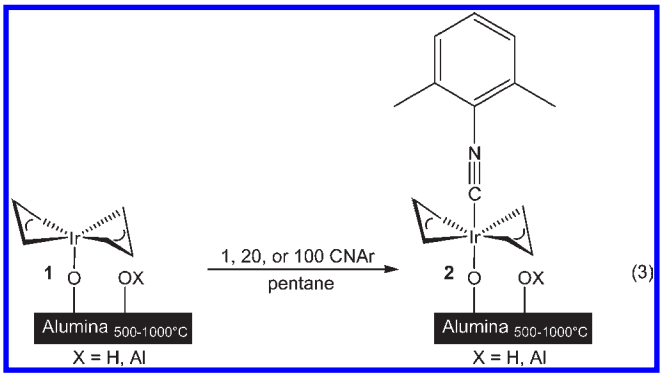

In the IR spectrum of **2**, a second much smaller isocyanide stretch was observed at 1989 cm^{-1}, regardless of the number of substrate equivalents added. To determine whether or not this lower-frequency stretch was due to isocyanide binding to Ir^0, a sample of **1** was prereduced under a constant flow of 6% H_2/94% Ar at 170 °C for 4 h, in an attempt to increase the ratio of Ir^0 to **2** present in the sample (see the decomposition studies in the following section). The subsequent addition of 20 equiv of 2,6-dimethylphenyl isocyanide to this sample (4 days at ambient temperature) significantly increased the ratio of the IR stretch at 1989 cm^{-1} relative to the stretch at 2132 cm^{-1} (Figure S2, Supporting Information), suggesting that the lower-frequency stretch is, in fact, due to isocyanide binding to Ir^0. Although this technique is not quantitative because each Ir^0 cluster may bind 1 equiv or more of isocyanide, the IR spectrum of **2** confirms that a small amount of Ir^0 is present in **1**.

The CP-MAS ^{13}C NMR spectrum of **2** was particularly valuable in determining the hapticity of the allyl ligands in this complex. In this spectrum, displayed in Figure 7, two distinct allyl ligand methylene resonances can be observed at 30.7 and 24.5 ppm, providing evidence that there are two inequivalent η^3-allyl methylene environments in **2** that are likely differentiated by the surface. The methine resonances associated with these ligands appear as an unresolved broad peak centered at 70.9 ppm. In addition, resonances for the bound isocyanide ligand were observed at 135.0 (aryl), 126.8 (aryl), and 18.2 ppm (methyl).

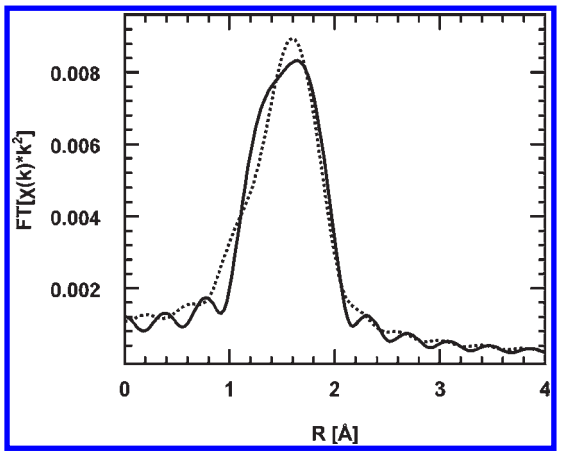

Figure 8. EXAFS data collected for complex **2** shown in *R*-space (solid line; without phase correction) along with the data fit (dashed line).

The EXAFS data collected on complex **2** were also reflective of 2,6-dimethylphenyl isocyanide ligation. The *R*-space data after Fourier transformation (not phase-corrected; solid line) are displayed in Figure 8, along with the fit, which is shown as a dashed line. The data fitting yielded an Ir−C/O coordination number of 3.4 at 2.02 Å (Table 1). This short average Ir−C/O bond distance reflects the binding of isocyanide to **1** because the Ir−CNAr distances in Ir(allyl)$_3$(CNAr)$_3$ were determined by X-ray crystallography to be an average of 1.979[5] Å.[30b] The Ir−C/O coordination number determined in this case is once again lower than expected because it was prepared directly from **1**.

The reaction of **1** with CO resulted in a different outcome than that observed upon 2,6-dimethylphenyl isocyanide addition. When an evacuated bomb containing **1** was charged with an atmosphere of CO and the gas was removed after 5 min at ambient temperature, the dicarbonyl complex (≡AlO)Ir(allyl)$_2$(CO)$_2$ (**3**; eq 4) was identified spectroscopically. The IR spectrum of this complex features symmetric and asymmetric CO stretching vibrations at 2068 and 1992 cm^{-1}, respectively (Figure 9, top). Upon labeling with ^{13}CO, these bands shift accordingly to 2020 and 1944 cm^{-1}, respectively. Unfortunately, this method of preparation is not a valid way to isolate this complex because only a small amount of **1** is converted to **3** under these conditions, as judged by CP-MAS ^{13}C NMR (29 200 scans needed to observe a weak carbonyl resonance for **3-^{13}CO**) and XAFS (sample nearly identical to the starting material).

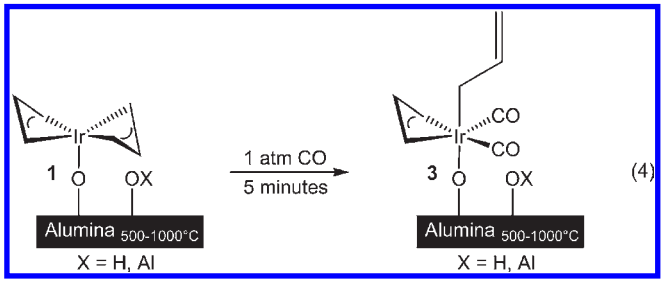

When **1** was exposed to an atmosphere of CO for more than 5 min, the alumina acquired a blue/green hue and the presence of a second carbonyl-containing species was detected by IR and CP-MAS ^{13}C NMR spectroscopies. As judged by IR spectroscopy, this newly formed moiety

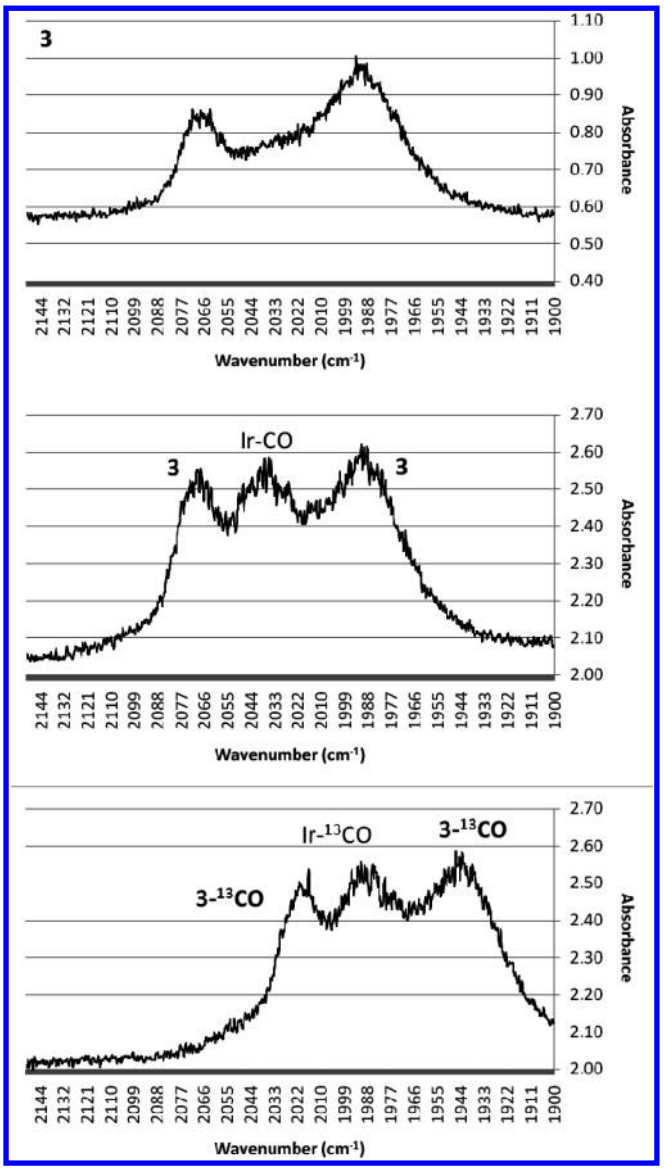

Figure 9. Solid-state IR spectrum of **3** after 5 min under an atmosphere of CO (top), shown along with spectra collected following exposure of **1** to an atmosphere of CO for 1 week (middle) and upon exposure of **1** to an atmosphere of ^{13}CO for 1 week (bottom). Ir−CO and Ir−^{13}CO represent the product of carbon monoxide addition to an Ir^0 cluster.

contains only one CO band at 2035 cm^{-1} (Figure 9, middle), which is consistent with that reported previously for ligation of CO to an Ir^0 cluster.[43] This band also shifted appropriately to 1988 cm^{-1} when ^{13}CO was employed (Figure 9, bottom). Preparing a mixture of complex **3-^{13}CO** with the newly formed Ir−^{13}CO species greatly facilitated the collection of CP-MAS ^{13}C NMR data. The equivalent, or nearly equivalent, carbonyl ligands in **3-^{13}CO** gave rise to a broad singlet centered at 161.0 ppm (Figure 10). Because this shift is similar to the one reported for the equivalent CO ligands in $Ir(allyl)_3(CO)_2$,[30b] these complexes have a similar electronic environment about the metal center, which also argues against the likelihood that **3** (or **1**) is cationic in nature. The ^{13}C NMR shift of the second carbonyl-containing species was also detected at 180.6 ppm.

(43) Zeinalipour-Yazdi, C. D.; Cooksy, A. L.; Efstathiou, A. M. *Surf. Sci.* **2008**, *602*, 1858–1862.

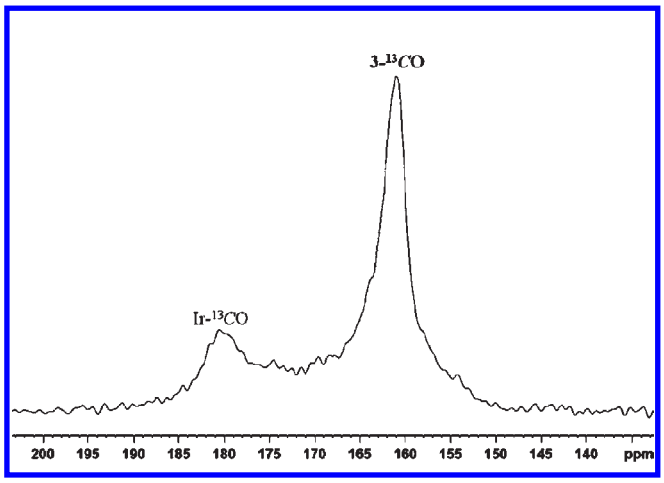

Figure 10. Mixture of **3-^{13}CO** and ^{13}CO adsorbed onto Ir^0 as observed by CP-MAS ^{13}C NMR spectroscopy, in ppm.

Although relatively intense spinning side bands from both Ir−^{13}CO resonances complicated the remainder of the NMR spectrum, resonances consistent with the presence of one η^1-allyl ligand (101.3 and 13.4 ppm) and one η^3-allyl ligand (70.2 and 24.5 ppm) were identified (see Figure S3 of the Supporting Information).

Exposure of **1** to an atmosphere of CO for periods of time longer than 1 week did not result in further conversion to Ir^0−CO. Additionally, placing the mixture of complexes under vacuum for 3 h did not increase the ratio of Ir^0−CO to **3** observed. The formation of Ir^0−CO also does not result from exposure of **3** to air or moisture because monitoring the IR spectrum of the mixture (or of **3** itself) in open air did not result in a change of the product ratio after 10 min. One approach in particular, the addition of $Ir(allyl)_3(CO)_3$[30b] to partially dehydroxylated γ-alumina, did improve the ratio of Ir^0−CO to **3**, although both products were still observed by IR spectroscopy. Within 2 h of mixing of the reagents, the slurry turned dark purple. After 4 days at ambient temperature, the reaction mixture was worked up and an olive-green solid was collected. As determined by IR spectroscopy, the change in the surface color from tan to purple, blue, or green appears to reflect the aggregation of iridium clusters *under ambient conditions*.

Alkane Dehydrogenation Experiments and Decomposition Studies. After the isolation and characterization of **1**, catalytic experiments were conducted to determine the viability of the supported bis(allyl)iridium complex to catalyze a series of alkane dehydrogenation transformations. Initially, turnover numbers greater than 100 h^{-1} were achieved when **1** was employed as the catalyst for the conversion of cyclohexane to benzene and of heptane to toluene at 200 and 270 °C, respectively.[44] However,

(44) In a typical dehydrogenation reaction, 30−50 mg of **1** was loaded into a 100 mL Schlenk tube containing 0.1 mL of an alkane substrate. The reaction vessel was then cooled to −78 °C, evacuated on a Schlenk line, sealed, and heated to either 200 or 270 °C for approximately 15 h. Upon completion of the reaction, the products were extracted into approximately 1 mL of CD_2Cl_2 and analyzed by ^{1}H NMR spectroscopy. In one trial, a turnover number of 121 for the dehydrogenation of cyclohexane to benzene was achieved at 200 °C (41% yield) when 0.050 g of **1** was employed as the catalyst. Using the same quantity of **1**, a turnover number of 156 was observed for the conversion of heptane to toluene at 270 °C (72% yield).

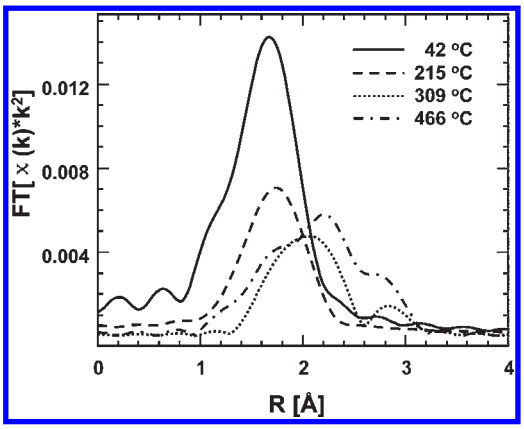

Figure 11. TPR of **1** under a flow of cyclohexane-saturated helium, as observed through in situ EXAFS measurements.

because high temperatures were required to effect these transformations and a lack of consistency in the turnover frequency was observed, it was hypothesized that the iridium nanoparticles rather than a well-defined immobilized iridium may be responsible for the observed catalysis.

In order to determine the true origin of this catalytic activity, a series of in situ XAFS experiments were conducted along with continuous-flow reactor studies. Because H_2 would inevitably be generated during catalytic alkane dehydrogenation, the stability of **1** under a flow of H_2 was investigated with ambient-temperature in situ XAFS measurements. However, only a slight reduction in the Ir−C coordination number was observed after approximately 15 min under a constant flow of 4% H_2/96% He with no observable metallic iridium. To more accurately mimic the conditions of the catalytic alkane dehydrogenation reactions, in situ temperature-programmed-reduction (TPR) experiments were conducted under a flow of cyclohexane gas in helium. This experiment revealed a clear decrease in the Ir−C coordination number and an increase in the Ir−Ir coordination number as a function of the temperature for **1** (Figure 11). The Ir−C coordination number decreased from approximately 6 to 3 upon heating from ambient temperature to 215 °C, with a further reduction in the Ir−C coordination number observed upon heating to 309 °C. Importantly, the formation of Ir−Ir contacts can be observed at 215 °C, providing evidence of additional Ir^0 nanoparticle formation under conditions that are milder than those employed in the catalytic alkane dehydrogenation reactions.[45]

In continuous-flow reactor studies, independently prepared batches of **1** were monitored for cyclohexane dehydrogenation activity in the temperature ranges of either 180−220 °C (Figure 12, dashed line) or 200−240 °C. In the lower-temperature trial, conversions of greater than 5% were never achieved. In the second trial, identical conversions were observed while heating from 200 to 220 °C, with conversions greater than 5% realized at 240 °C. In a third trial, a sample of **1** (same iridium loading as that in trial 1) was treated at 370 °C for 1 h with

(45) Because the catalytic trials were conducted in a closed system, a buildup of H_2 pressure in the reaction vessel would result in more reducing conditions than those in the in situ XAFS experiments, which were conducted under a constant flow of cyclohexane gas in helium.

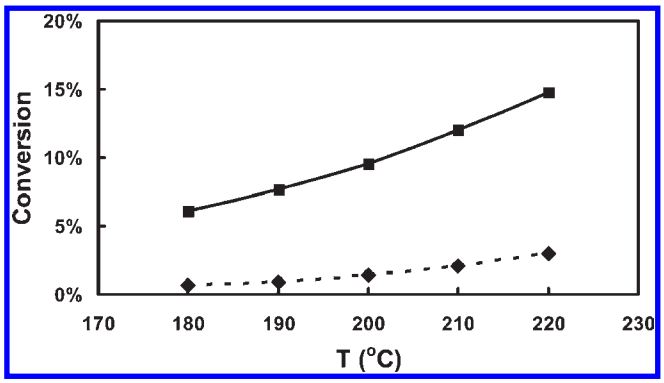

Figure 12. Percent conversion of cyclohexane dehydrogenation as a function of the temperature for **1** (dashed line) and preformed Ir^0 (solid line).

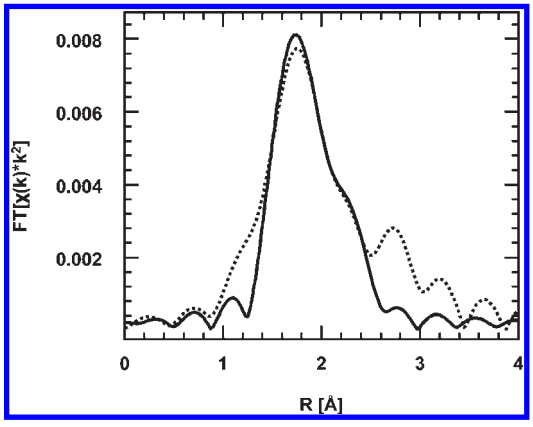

Figure 13. *R*-space EXAFS plot (not phase-corrected) of **1** after heating to 240 °C under a cyclohexane/argon flow (solid line). Fitted data are presented as a dashed line.

Table 3. EXAFS Fitting Results of **1** upon Completion of the Continuous-Flow Reactor Study

complex	scatter	CN (±20%)	*R* (±0.02 Å)	DWF (Å^2 × 10^3)	E_0 (eV)
1 (240 °C)	Ir−C	3.1	2.12	5.9	5.4
	Ir−Ir	2.4	2.77	2.0	2.8

a flow of 5% H_2 in argon, conditions under which **1** would be fully reduced to Ir^0. The activity observed for the prereduced sample (Figure 12, solid line) was significantly higher (∼15% conversion at 220 °C) than the activity observed using unreduced **1** under the same reaction conditions, providing a second line of evidence that the alkane dehydrogenation reactions were catalyzed predominantly by Ir^0 nanoparticles rather than a well-defined monometallic species.

Upon completion of the second trial of the reactor conversion study (heating from 200 to 240 °C), the iridium catalyst **1** was collected without exposure to air and an XAFS measurement was taken. After Fourier transformation, a clearly defined Ir−Ir shoulder was observed to the right of the Ir−C/O peak (Figure 13). EXAFS data analysis revealed the formation of 2.4 Ir−Ir contacts at 2.77 Å during the course of the catalytic reaction (Table 3). This measurement provides direct evidence that additional iridium nanoparticles are, in fact, formed under the alkane dehydrogenation conditions and that they are the most active species.

Discussion and Comparison to Rh(allyl)$_3$ Immobilization Studies. Because the reactivity of (≡SiO)(≡SiOX)Rh(η^3-allyl)$_2$ (X = H, Si) toward Lewis bases such as phosphines and CO has been thoroughly investigated,[32] comparisons between the immobilized bis(allyl)rhodium and iridium systems warrant discussion. The reactivity observed for (≡SiO)(≡SiOX)Rh(η^3-allyl)$_2$ was found to vary greatly with the degree of support dehydroxylation. For example, when excess CO was added to the rhodium complex supported on silica that was partially dehydroxylated at 550 °C, reductive elimination of 1,5-hexadiene was observed along with a small amount of 1,6-heptadien-4-one and a species proposed to be the surface-bound rhodium dimer, [(≡SiO)Rh(CO)$_2$]$_2$.[32a] However, when the silica was partially dehydroxylated at 200 °C, the binding of 3 equiv of CO and liberation of 1 equiv of propene were observed, affording a species proposed to be (≡SiO)$_2$Rh(CO)$_3$(η^1-allyl).[32a] Both this product and its proposed phosphine-ligated analogue, (≡SiO)$_2$Rh(PMe$_3$)$_3$(η^1-allyl), exhibited poor redox stability because either acyl (following CO insertion) or allyl group transfer to the surface was observed, respectively.[32a]

The reactivity studies on the rhodium system highlight the importance of achieving a good degree of surface homogeneity prior to metal complex immobilization. For the immobilization of Ir(allyl)$_3$ discussed in this manuscript, the relative inertness of this complex, when compared to that of Rh(allyl)$_3$, prevented the immobilization reaction from taking place between Ir(allyl)$_3$ and silica. In turn, we chose highly Brønsted acidic, partially dehydroxylated γ-alumina as the support. Unfortunately, this support bears microenvironments that are much more reactive than similar sites on a silica surface, a factor that undoubtedly contributed to small amounts of Ir^0 formation during the immobilization of Ir(allyl)$_3$.

The observation that allyliridium complexes are more stable toward redox events than their rhodium counterparts in solution[30b,33] also carried over to the site-isolated reactivities of these complexes. For example, when **1** was subjected to an atmosphere of CO over the course of a week, no evidence for CO insertion was observed by IR and the resulting dicarbonyl **3** was remarkably stable, even upon exposure to air. Although this inherent robustness could prove invaluable for the discovery of well-defined complexes that can function as catalysts at high temperatures, better methods of tethering these allyliridium complexes to a surface will need to be developed. Future studies in this regard will focus on the pretreatment of alumina-based surfaces in an attempt to saturate the highly reactive alumina microenvironments that appear to contribute to Ir^0 formation. The addition of iridium complexes bearing chelating ligands to highly acidic surfaces may also prove to be valuable in circumventing metallic iridium formation.

Concluding Remarks

A series of γ-alumina-supported iridium complexes were characterized by a suite of techniques including XAFS, IR, and solid-state NMR spectroscopy. Although a highly acidic support was required for the covalent attachment of Ir(allyl)$_3$ to the surface, this characteristic also contributed to the undesired deposition of small amounts of zerovalent iridium during the immobilization reaction. TPR of the supported bis(η^3-allyl)iridium complex revealed that its integrity was slowly compromised at temperatures above 150 °C, rendering it inadequate for high-temperature catalytic studies. On the other hand, because this complex proved more resistant to redox changes than its well-studied rhodium congener, the potential remains that the covalent immobilization of judiciously selected Ir^{3+} complexes to a surface may lead to the development of well-defined alkane dehydrogenation catalysts.

Experimental Section

General Considerations. All synthetic reactions were performed in an MBraun glovebox under an atmosphere of purified nitrogen. Aldrich or Acros anhydrous solvents were sparged with argon and stored in the glovebox over activated 4 Å molecular sieves and sodium before use. Benzene-d_6 and methylene chloride-d_2 were purchased from Cambridge Isotope Laboratories and dried over 4 Å molecular sieves prior to use. Triphenylphosphine, dimethylphenylphosphine, and ferrocene were used as received from Acros, while cyclohexane, heptane, and boron nitride were purchased from Aldrich and dried before use. All of the gases used in this study were obtained from Airgas with the exception of ^{13}CO, which was purchased from Cambridge Isotope Laboratories. Several of the allyliridium complexes studied in this manuscript, including Ir(allyl)$_3$, Ir(η^3-allyl)$_2$(η^1-allyl)(PPh$_3$), Ir(η^3-allyl)(η^1-allyl)$_2$(κ^2-Ph$_2$PC$_6$H$_4$PPh$_2$), Ir(η^1-allyl)$_3$(κ^3-Ph$_2$P(CH$_2$)$_2$P(Ph)(CH$_2$)$_2$PPh$_2$), and Ir(allyl)$_3$(CO)$_3$, were prepared according to literature procedures.[30b] The tied-back phosphite, P(OCH$_2$)$_3$CCH$_3$, was also prepared according to a literature procedure.[46] Solution ^{1}H NMR spectra were recorded at room temperature on a Bruker AVANCE 400 MHz spectrometer. All ^{1}H and ^{13}C NMR chemical shifts are reported relative to SiMe$_4$ using ^{1}H (residual) and ^{13}C chemical shifts of the solvent as secondary standards. ^{31}P NMR data are reported relative to H$_3$PO$_4$. IR spectra of the supported iridium complexes were recorded on a Thermo Nicolet Nexus 470 FT-IR spectrometer running *OMNIC* software. ICP mass spectrometry (ICP-MS) experiments were conducted on a Varian MPX Simultaneous ICP-AES instrument, following EPA SW 846 Method 6010. Elemental analyses were performed at Atlantic Microlab, Inc., in Norcross, GA.

Solid-State NMR Measurements. Solid-state CP-MAS NMR experiments were conducted on a Bruker AVANCE system with the resonance frequency of ^{13}C at approximately 100.6 MHz. Experiments were typically performed on 50−75 mg of solid material packed under argon in airtight 4 mm rotors. The $\pi/2$ pulse for ^{1}H was 4.00 μs, and the Hartmann−Hahn match condition was optimized for a 4 mm rotor at a spinning speed of 10 000 Hz. The contact time for magnetization transfer was 5 ms, and the relaxation delay between scans was 3 s. Approximately 4000 acquisitions were necessary for the Ir(allyl)$_3$ sample, 100 000 for **1**, 140 000 for **2**, and 66 000 for **3-^{13}CO**. Additionally, CP-MAS ^{31}P NMR spectroscopy was utilized as a probe for Lewis base reactivity toward **1**.

Support Activation. γ-Alumina (Strem Chemical, 97%) was activated under flowing gas using a standard tube furnace prior to employment in the immobilization reactions. Approximately 2.5 g of γ-alumina was placed in a quartz tube, a flow of helium was established, and the solid was heated at either 500 or 1000 °C for 20 min to yield partially dehydroxylated γ-alumina.[34] Immediately following activation, the alumina was quickly transferred to the glovebox and stored in a sealed container under dinitrogen.

(46) Wadsworth, W. S., Jr.; Emmons, W. D. *J. Am. Chem. Soc.* **1962**, *84*, 610–617.

Preparation of (≡AlO)Ir(allyl)$_2$ (1). In the glovebox, a 20 mL scintillation vial was charged with 0.570 g of γ-alumina (partially dehydroxylated at either 500 or 1000 °C, as described above), 0.013 g (0.041 mmol) of freshly sublimed Ir(allyl)$_3$, and approximately 5 mL of pentane. The slurry was set to stir at ambient temperature, and a color change from white to light tan was observed over the course of 24 h. After 3 days, the reaction mixture was filtered and the isolated tan solid was washed five times with approximately 10 mL of pentane to remove any residual Ir(allyl)$_3$. Upon drying in vacuo, 0.505 g (~88% yield) of **1** was collected. Removal of pentane from the filtrate allowed re-collection of approximately 20% of the original Ir(allyl)$_3$, as judged by ^{1}H NMR spectroscopy upon integration against a known quantity of ferrocene. Using a modified procedure, a solution of 0.003 g (0.01 mmol) of Ir(allyl)$_3$ and 0.002 g (mmol) of ferrocene in 1.5 mL of toluene-d_8 was added to a J. Young NMR tube that was preloaded with 0.600 g of partially dehydroxylated γ-alumina (1000 °C). After 5 h, the evolved propene was quantified by ^{1}H NMR spectroscopy, upon integration against the added ferrocene. The iridium loading was determined to be between 1.2 and 1.6 wt % by ICP-MS, depending on the batch of partially dehydroxylated γ-alumina employed. CP-MAS ^{13}C{^{1}H} NMR: δ 70.6 (CH_2CHCH_2), 24.6 (CH_2CHCH_2).

EXAFS Measurements. In situ H_2 and cyclohexane TPR EXAFS studies of **1** at the Ir L_3 edge were performed at the Materials Research Collaborative Access Team (MRCAT) and CMC beamlines at the Advanced Photon Source, Argonne National Laboratory. The setup used was similar to that outlined by Castagnola et al.[47] In an argon-filled Vacuum Atmospheres glovebox with a large-capacity recirculator (0.25 ppm of O_2 and 0.5 ppm of H_2O), approximately 25 mg of each sample was loaded as a self-supporting wafer without binder in the channels (i.d. = 4 mm) of a stainless steel multisample holder. The sample holder was then placed in the center of a quartz tube, which was equipped with gas and thermocouple ports and Kapton windows. The amount of sample used was optimized for the Ir L_3 edge, considering absorption by the aluminum in the support. With the gas ports closed, the setup was transferred into the experiment hutch. The quartz tube was placed in a clamshell furnace, and both were mounted on a positioning platform. Helium flow at 200 mL/min was established to remove the residual argon. The beam was set to scan the sample cell holder by manipulating the position of the platform. Once the sample positions were fine-tuned, the reactant gas (4% H_2 in helium or cyclohexane-saturated helium) was flowed through the samples (50 mL/min) and a temperature ramp of 2 °C/min was initiated for the furnace. The EXAFS spectra were recorded in transmission mode, and a platinum foil spectrum was measured simultaneously with each sample spectrum for energy calibration purposes. Spectra for each sample were collected from 11 000 to 12 258 eV, with a step size of 0.45 eV and an acquisition time of 0.03 s/step. The change in the sample temperature from the absorption edge through the end of the scan was approximately 2.8 °C, while each sample was probed approximately every 15 °C. On the basis of the observed temperature dependence of the transitions, the local structure remains essentially the same throughout a single spectrum from the absorption edge to the end of the scan.

XAFS Data Analysis. Because iridium is next to platinum in the periodic table, phase shifts and backscattering amplitudes of Pt−Pt and Pt−N scattering, which were obtained from a platinum foil and $Pt(NH_3)_4Cl_2$, respectively, were utilized for Ir−Ir and Ir−C contributions, respectively. Standard procedures based on *WINXAS 3.1* software were used to fit the XAS data. XANES spectra of the supported iridium catalyst under various conditions were fitted as linear combinations of the XANES spectra of Ir(allyl)$_2$(O−)/Al_2O_3 and fully reduced Ir^0/Al_2O_3. The EXAFS coordination parameters were obtained by a least-squares fit in the q and r spaces of the isolated nearest-neighbor, k^2-weighted Fourier transform data. The quality of the fits was equally good with both k^1- and k^3-weightings.

Preparation of Ir(η^3-allyl)(η^1-allyl)$_2$(PMe$_2$Ph)$_2$ (C). In the glovebox, a 20 mL scintillation vial was charged with 0.100 g (0.317 mmol) of Ir(allyl)$_3$ and approximately 3 mL of toluene. While stirring, a second solution of 0.087 g (90 μL, 0.633 mmol) of dimethylphenylphosphine in approximately 3 mL of toluene was added. The solution became yellow over the course of 2.5 h at ambient temperature. At this point, the solvent was removed in vacuo to yield a yellow oil. This oil was redissolved in pentane, and the solvent was evacuated several times until 0.114 g (61%) of a yellow solid identified as **C** was collected. Anal. Calcd for $C_{25}H_{37}IrP_2$: C, 50.74; H, 6.30. Found: C, 50.61; H, 6.17. ^{1}H NMR (benzene-d_6): δ 7.18 (m, 2H, *phenyl*), 7.07−6.96 (m, 8H, *phenyl*), 5.68 (overlapping m, 2H, CH_2CH=CH_2), 4.89 (dd, J_{HH} = 10.0 and 2.5 Hz, 1H, CH_2CH=CH_2), 4.68 (m, 3H, CH_2CH=CH_2), 3.85 (quintet, J_{HH} = 9.0 Hz, 1H, CH_2CHCH_2), 2.69 (m, 2H, CH_2CHCH_2), 2.23 (m, 2H, CH_2CHCH_2), 1.85 (m, 2H, CH_2CH=CH_2), 1.35 (d, J_{HP} = 8.5 Hz, 6H, PPh(CH_3)$_2$), 1.29 (d, J_{HP} = 8.5 Hz, 6H, PPh(CH_3)$_2$). ^{13}C{^{1}H} NMR (benzene-d_6): δ 148.9 (t, $^4J_{CP}$ = 3.0 Hz, CH_2CH=CH_2), 147.6 (t, $^4J_{CP}$ = 3.0 Hz, CH_2CH=CH_2), 141.1 (dd, $^2J_{CP}$ = 43.0 Hz, $^4J_{CP}$ = 3.0 Hz, *1-phenyl*), 130.1 (d, $^3J_{CP}$ = 9.0 Hz, *2-phenyl*), 129.0 (s, *phenyl*), 128.3 (s, *phenyl*), 110.4 (s, CH_2CHCH_2), 105.2 (s, CH_2CH=CH_2), 105.1 (s, CH_2CH=CH_2), 48.8 (dd, $^3J_{CP\text{-}trans}$ = 33.0 Hz, $^3J_{CP\text{-}cis}$ = 2.5 Hz, CH_2CHCH_2), 14.8 (d, $^2J_{CP}$ = 33.5 Hz, PPh(CH_3)$_2$), 14.6 (d, $^2J_{CP}$ = 33.5 Hz, PPh(CH_3)$_2$), 0.8 (t, $^3J_{CP}$ = 4.5 Hz, CH_2CH=CH_2), −1.2 (t, $^3J_{CP}$ = 5.0 Hz, CH_2CH=CH_2). ^{31}P{^{1}H} NMR (benzene-d_6): δ 39.5 (s).

Preparation of (≡AlO)Ir(allyl)$_2$(CNAr) [2; Ar = 2,6-(CH$_3$)$_2$-C$_6$H$_4$]. In the glovebox, a 20 mL scintillation vial was charged with 0.200 g of **1** and 0.034 g (0.258 mmol, 20 equiv) of 2,6-dimethylphenyl isocyanide. Upon the addition of approximately 5 mL of pentane, the solid immediately changed from light tan to yellowish-orange. The resulting slurry was allowed to stir for 3 days at ambient temperature before the light-orange solid was collected via filtration. This solid was washed twice with 10 mL of toluene and then twice with 10 mL of pentane. Upon drying, 0.183 g (~91%) of **2** was obtained. The iridium loading in **2** was determined to be 1.6% by ICP-MS. CP-MAS ^{13}C{^{1}H} NMR: δ 135.0 (*aryl*), 126.8 (*aryl*), 70.9 (π-*allyl*), 30.7 (π-*allyl*), 24.5 (π-*allyl*), 18.7 (CH_3). IR (solid state): ν_{CN} 2132 cm^{-1}.

Observation of (≡AlO)Ir(allyl)$_2$(CO)$_2$ (3). In the glovebox, a thick-walled glass vessel was charged with 0.160 g of **1** and sealed. The bomb was evacuated on a Schlenk line and then charged with 1 atm of CO. After 5 min, the CO atmosphere was evacuated, the vessel was brought back into the glovebox, and 0.106 g of CO-modified **1** was collected. Upon spectroscopic investigation, this material was found to contain small amounts of **3**. IR (solid state): ν_{CO} 2068, 1992 cm^{-1}. A similar procedure was used to prepare the ^{13}CO-labeled version of this complex at early reaction times (**3-^{13}CO**). IR (solid state): $\nu^{13}{}_{CO}$ 2020, 1944 cm^{-1}. Allowing the reaction between **1** and ^{13}CO to remain at ambient temperature for 24 h rather than 5 min allowed greater conversion to **3-^{13}CO**, which could then be characterized by CP-MAS ^{13}C NMR spectroscopy. CP-MAS ^{13}C{^{1}H} NMR: δ 161.0 (s, ^{13}*C*O), 101.3 (σ-*allyl*), 70.2 (π-*allyl*), 24.5 (π-*allyl*), 13.4 (σ-*allyl*). A small amount of this complex was also identified by IR spectroscopy upon mixing of a toluene solution containing 0.007 g (0.017 mmol) of Ir(allyl)$_3$(CO)$_3$ with 0.400 g of partially dehydroxylated γ-alumina for 4 days. Within 2 h of mixing the reactants, the slurry turned dark purple and turned olive green over the course of the reaction because of the formation of CO-ligated Ir^0 clusters, which were identified as the major product by IR spectroscopy. IR (solid state): ν_{CO} 2035 cm^{-1}.

(47) Castagnola, N. B.; Kropf, A. J.; Marshall, C. L. *Appl. Catal., A* **2005**, *290*, 110–122.

Cyclohexane Dehydrogenation Reactor Studies. In an argon-filled Vacuum Atmospheres glovebox with a large capacity recirculator (0.25 ppm of O_2 and 0.5 ppm of H_2O), a predetermined amount of **1** was loaded into a $^1/_2$-in. quartz tube reactor equipped with an Omega K-type thermocouple and two on/off valves. With argon purging, the reactor assembly was attached to a catalyst testing unit and the catalyst bed was positioned at the center of a clamshell furnace. The gas flow rates were controlled by Brooks Instrument 5850E mass flow controllers. Cyclohexane was fed by flowing reaction gas (argon) through a cyclohexane bubbler kept at room temperature. The effluent gas from the reactor was analyzed with an online Hewlett-Packard 5890 series II Plus gas chromatograph equipped with a HayeSep D column, an Alltech-washed 5 Å molecular sieve column, and a thermal conductivity detector, which had been calibrated for hydrogen, cyclohexane, cyclohexene, cyclohexadiene, and benzene. Organic products were trapped in a chilled receiver and later were subjected to gas chromatography−mass spectrometry analysis.

Preparation of Supported Zerovalent Iridium. In an argon-filled Vacuum Atmospheres glovebox with a large-capacity recirculator (0.25 ppm of O_2 and 0.5 ppm of H_2O), 158 mg of **1** was loaded into a $^1/_2$-in. quartz tube reactor equipped with an Omega thermocouple and on/off valves. With argon purging, the reactor assembly was attached to the catalyst testing unit. The catalyst was treated with 5% H_2 in argon at 370 °C for 1 h, under which the supported Ir^{3+} was reduced to Ir^0.

Acknowledgment. We thank the Office of Basic Energy Sciences, Division of Chemical Sciences, Geosciences, and Biosciences, for financial support through the Catalysis Science Program. Use of the Advanced Photon Source was also supported by the Office of Basic Energy Sciences of the U.S. Department of Energy under Contract DE-AC02-06CH11357. MRCAT (Sector 10) operations are supported by the Department of Energy and the MRCAT member institutions. The collection of XAFS data was also carried out at the XOR Beamlines (Sector 9), which are supported in part by the Office of Basic Energy Sciences of the U.S. Department of Energy and by the National Science Foundation Division of Materials Research. We thank Drs. Jeremy Kropf and Trudy Bolin for assistance with the collection of XAFS measurements and Brandy Duran for conducting ICP-MS experiments. We are also grateful to Drs. Worajit Setthapun and Weiling Deng for helpful discussions involving the continuous flow reactor studies. LANL is operated by Los Alamos National Security, LLC, for the National Nuclear Security Administration of the U.S. Department of Energy under contract DE-AC52-06NA25396.

Supporting Information Available: Stoichiometric propene determination and IR, NMR, and EXAFS spectra. This material is available free of charge via the Internet at http://pubs.acs.org.